LETTERS TO THE EDITOR

To the Editor:

Kuo and Chou [**34**(6), 1304, June, 1988], as an integral part of their paper titled, "Benzaldehyde Oxidation Catalyzed by the Wall of a Tubular Bubble Column Reactor," present some useful, but uncorrelated, experimental data for axial dispersion coefficient vs. superficial gas velocity. The data are quite useful, since a solvent (acetone at 15°C) other than water was used. Moreover, the values reported were quite small, in agreement with predictions published in a recent theory by Rice and Littlefield (1987). This work suggested that the proper turbulence length scale for truly vertical bubble columns with high quality spargers should be bubble size, rather than the column diameter used originally by Baird and Rice (1975) in their so-called isotropic, homogeneous turbulence model. Kuo and Chou did not report, or comment on, observed bubble sizes, but their holdup curve given as Figure 2 allows a first estimate of this important quantity. Thus, if we write the slip velocity for batch columns to be related to gas voidage as:

$$U_s = \frac{U_g}{\epsilon} = U_\infty (1 - \epsilon)^{n-1} \quad (1)$$

then their Figure 2 allows an estimate of single-bubble rise, taking $n = 3$ according to Rice and Littlefield, to be:

$$U_\infty = \frac{1 \text{ cm/s}}{(0.09)(1 - 0.09)^2} = 13.4 \text{ cm/s} \quad (2)$$

Moreover, it was shown by the latter authors that a linear connection between U_∞ and bubble size (d_B) existed for the intermediate Reynolds number region:

$$d_B \sim U_\infty \left[\frac{15\,\nu^{1/2}}{2g}\right]^{2/3} \quad (3)$$

At 15°C we can estimate the kinematic liquid acetone viscosity to be $\nu = (0.355/0.791) \times 10^{-2}$ cm^2/s, so that Eq. 2 and 3 yield the forecast:

$$d_B \sim 0.086 \text{ cm} \quad (4)$$

The above information allows the axial dispersion coefficient to be estimated from the Rice-Littlefield relation:

$$D_{Be} = (d_B)^{4/3} (U_g \cdot g)^{1/3} \quad (5)$$

Taking $U_g \sim 1$ cm/s, yields the prediction:

$$D_{Be} = 0.38 \text{ cm}^2/\text{s} \quad (6)$$

which compares favorably with Kuo and Chou's Figure 3, i.e., $D_e^* \sim 0.72$ cm^2/s.

Predictions from the original Baird-Rice theory using column diameter as length scale, can be computed from:

$$D_{ce} = 0.35 (d_c)^{4/3} (U_g \cdot g)^{1/3} \quad (7)$$

which, for the Kuo-Chou column ($d_c \sim 2.7$ cm), yields the forecast for the same U_g:

$$D_{ce} = 13 \text{ cm}^2/\text{s} \quad (8)$$

which is more than an order larger than the acetone results reported by these workers.

Our recent experiments (Barbe, 1988) using the colorful acid-base method of Littlefield (1986), suggest that two turbulence length scales are operative in vertical bubble columns:

- Near the sparger, in the lower reaches of the column, the scale is column diameter.
- In the upper reaches, the scale changes to a length proportional to bubble size.

To sum up these effects, we can postulate that the overall coefficient obeys the rule:

$$\frac{L}{D_{oe}} = \frac{L_c}{D_{ce}} + \frac{(L - L_c)}{D_{Be}} \quad (9)$$

where D_{ce} and D_{Be} are eddy coefficients corresponding to length scales d_c and d_B, respectively. For the Kuo-Chou column of length 135 cm, supposing we assume mixing zones of equal length (Barbe, 1988), we have

$$\frac{135}{D_{oe}} = \frac{67.5}{13} + \frac{67.5}{0.38} \quad (10)$$

which predicts

$$D_{oe} \sim 0.74 \text{ cm}^2/\text{s} \quad (11)$$

This is very close indeed to the experimental value reported earlier ($D_e^* \sim 0.72$ cm^2/s).

While it is unclear at this point how to predict the entrance length, L_c, precisely, for (apparently) bubble flow conditions, nonetheless we find evidence that $L_c \sim 0.5\,L$ for water columns much larger than used by Kuo and Chou.

Researchers are encouraged to exploit the summation rule, Eq. 9, in an effort to help unify the disparate literature data on bubble column mixing.

Notation

d_B = bubble diameter, cm
d_c = column diameter, cm
D_e^* = experimental eddy dispersion coeff. cm^2/s
D_{oe} = overall eddy dispersion coeff., cm^2/s

D_{Be} = eddy coeff. based on bubble diameter, cm^2/s
D_{ce} = eddy coeff. based on column diameter, cm^2/s
L = column length, cm
L_c = entrance length, cm
n = Richardson-Zaki exponent
U_g = superficial gas velocity, cm/s
U_s = slip velocity, cm/s
U_∞ = terminal rise velocity of single bubble, cm/s
ϵ = gas voidage
ν = liquid kinematic viscosity, cm^2/s

Literature cited

Baird, M. H. I., and R. G. Rice, "Axial Dispersion in Large Unbaffled Columns," *Chem. Eng. J.*, **9**, 171 (1975).

Barbe, D. T., personal communication (1988).

Kuo, M. C., and T. C. Chou, "Benzaldehyde Oxidation Catalyzed by the Wall of a Tubular Bubble Column Reactor," *AIChE.*, **34**, 1034 (1988).

Littlefield, M. A., "Determination of Dispersion Coefficients in a Bubble Column by an Acid-Base Neutralization Method," M.S. Thesis, Lousiana State Univ. (1986).

Rice, R. G., and M. A. Littlefield, "Dispersion Coefficient for Ideal Bubbly Flow in Truly Vertical Bubble Columns," *Chem. Eng. Sci.*, **42**, 2045 (1987).

Richard G. Rice
Dept. of Chemical Engineering
Lousiana State University
Baton Rouge, LA 70803

To the Editor:

Leighton and McCready, in their paper titled, "Shear Enhanced Transport in Oscillatory Liquid Membranes," [34 (10) 1709, October, 1988], present an idea whereby oscillatory fluid motion is predicted to enhance transport in liquid membranes. This idea is not new and key references (Horn and Kipp, 1967; Harris and Goren, 1967) are missing. They state ". . . the substantial degree of selectivity which can occur has apparently not been previously realized." As a matter of fact, Rice and Eagleton (1970) showed in their Figure 7 a clear selective separation by comparing two species undergoing stationary oscillatory flow; the species Schmidt numbers were 1,000 and 100, respectively. Moreover, Rice (1974), based on experiments on actual porous media, reported enhancements up to 450% relative to simple liquid diffusion in pores.

It is clear that all of the major points raised in this paper have already been published, including single species enhancement, species selectivity and actual experiments in porous media.

Literature cited

Harris, H. G., and S. L. Goren, "Axial Diffusion in a Cylinder with Pulsed Flow," *Chem. Eng. Sci.*, **22**, 1571 (1967).

Horn, F. J. M., and K. L. Kipp, "Mass Transport under Oscillating Flow Conditions," *Chem. Eng. Sci.*, **22**, 1869 (1967).

Rice, R. G., and L. C. Eagleton, "Mass Transfer Produced by Laminar Flow Oscillations," *Can. J. Chem. Eng.*, **48**, 46 (1970).

Rice, R. G., "Effect of Fluid Oscillations on Mass Transfer in Porous Media with Particular Reference to Porous Electrode Fuel Cells," Proc. Australasian Conf. on Hydraul. and Fluid Mech., Christcurch, New Zeland **11**, 238 (1974).

Richard G. Rice
Dept. of Chemical Engineering
Louisiana State University
Baton Rouge, LA 70803

Reply:

We are indebted to Professor Rice for pointing out to us the literature references on oscillating flow through tubes which we had missed during our literature search. While Rice and Eagleton (1970) did note in their paper that the enhancement of mass transport was greater for species with smaller diffusivities, this had been previously recognized by Horn and Kipp (1967) for the similar system of an oscillating Couette flow. The novelty of our paper, which is reflected by the title, "Shear Enhanced Transport in Oscillatory Liquid Membranes," is the intended application which addresses specific difficulties with current liquid membrane designs, e.g., slow transport rates and lack of selectivity with respect to solvent molecules. As mentioned in our paper, our calculations were obtained by a straightforward application of the results of Aris (1960), Harris and Goren (1967), and Watson (1983) (the first and last of which we did reference) and were used to demonstrate the usefulness of the intended applications. We have subsequently verified this application by obtaining a thirty-fold enhancement in mass transport for a model liquid membrane system. The results of these experiments were presented at the Washington AIChE meeting (paper 2b).

Literature cited

Aris, R., "On the Dispersion of a Solute in Pulsating Flow through a Tube," *Proc. Roy. Soc. A*, **259**, 370 (1960).

Leighton, D. T., and M. J. McCready, "Shear Enhanced Transport in Oscillatory Liquid Membranes," paper 2b, AIChE Meeting, Washington, DC (1988).

Watson, E. J., "Diffusion in Oscillatory Pipe Flow," *J. Fluid Mech.*, **133**, 233 (1983).

David T. Leighton
Mark J. McCready
Dept. of Chemical Engineering
Univ. of Notre Dame
Notre Dame, IN 46556

Table 1. Comparison of Parameter Estimates

	Simulation Example*	Glauber Salt Example**
Linear Least Squares (Estimates)		
$G \times 10^8$ (m/s)	5.5	2.56
$n^o \times 10^{-10}$ (n^o/m · kg)	1.0	51.2
e_p (%)	3.5×10^{-12}	24.1
e_{pl} (%)	2.6×10^{-13}	1.1
e_w (%)	8.7×10^{-13}	36.1
Tangency Method**		
$G \times 10^8$ (m/s)	5.5	2.57
$n^o \times 10^{-10}$ (n^o/m · kg)	1.0	44.6
e_p (%)	3.5×10^{-12}	22.7
e_{pl} (%)	2.6×10^{-13}	1.2
e_w (%)	8.7×10^{-13}	36.2
Weight Mean Method		
$G \times 10^8$ (m/s)	4.9	2.57
$n^o \times 10^{-10}$ (n^o/m · kg)	1.6	44.6
e_p (%)	33.4	22.7
e_{pl} (%)	1.2	1.2
e_w (%)	23.0	36.2

*Exact population density, Eq. 1: τ = 5,400 s; M_T = 0.405 kg/kg; $\rho_c k_v$ = 0.833 kg/L; ρ_L = 1 kg/L
**From White and Randolph (1987): τ = 5,400s; M_T = 0.3 kg/kg; $\rho_c k_v$ = 0.81 kg/L; ρ_L = 1 kg/L (assumed)

To the Editor:

White and Randolph (1987) presented a method of incorporating the material balance (or self-consistency check) into the semilog plotting method for mixed suspension mixed product removal (MSMPR) crystallizers in order to extract consistent and accurate estimates of growth rate (G) and nuclei population density (n^o). In their procedure, the product crystal size distribution (CSD) data from an MSMPR crystallizer are plotted on semilog paper either as the specific population density $(n\rho_c k_v)/(M_T)$ or specific cumulative number oversize $(N\rho_c k_v)/(M_T)$. A tangent to the tangency curve, best fitting the experimental data, is then selected to estimate the best values of the mean size ($\bar{L} = G\tau$). The points of tangency are around L = four $\bar{L}$ for specific population density and $L = 3\bar{L}$ for specific cumulative number oversize. Once the estimate of $\bar{L}$ is obtained, n^o is then determined from the suspension density (M_T).

Although a number of modifications for parameter estimation procedure with an MSMPR crystallizer have been suggested, three techniques, *viz.*, linear least squares, the tangency method and weight mean size, will be used here for illustration purposes. Two illustrative examples are taken; first a simulation, and second, Glauber Salt Crystallization using data of White and Randolph (1987). In the simulation example, 22 data points were taken from the exact population density curve described by:

$$n = 10^{10} \exp\left(-\frac{L}{3.0 \times 10^{-4}}\right) \quad (1)$$

Points at the midsizes of British Standard sieves over the size range 41–1,840 μm were used to simulate the product population density data. In the linear least squares technique, a regression analysis of the data points was performed for the linearized equation of population density function in natural log variables. In the weight mean size procedure the growth rate was determined from the weight mean size of the product crystals using $\bar{L}_w = 4G\tau$ and nuclei population density from the magma density. The results of parameter estimates and ratios of moments are reported in Tables 1 and 2, respectively.

The material balance constraint, which demands that the measured magma density of product crystals equal the magma density calculated from the change between inlet and outlet solute concentrations, is generally satisfied within the limits of experimental accuracy. However, the magma density calculated theoretically using kinetic information may not necessarily match the measured magma density. In both the tangency and weight mean size methods the nuclei population density is determined from a rather weak definition derived from a relation linking the third moment of the expected experimental distribution to the measured suspension density. The size analysis technique may not be applicable over the entire size range of product crystals and may yield large errors on either end of the measured size range. The weight density function as shown in Figure 1, together with the population density data, may perhaps provide consistent estimates of kinetic rates rather than the (specific) population density data alone. The results in Table 2 do not precisely reflect the internal consistency of the product size distributions, as the simulation example sets the limits on accuracy. In order to gain confidence for the description of a process configuration, the consistency on both solution and solid side information is important. It is also difficult to achieve complete satisfactory consistency and to

Table 2. Ratio of Moments

Ratio of Moments $\times 10^6$, m	Simulation Example Calculated from		Glauber Salt Example* Calculated from	
	Eq. 1	Simulated Data	Parameters**	Exp. Data
μ_1/μ_0	300	335	139	261
μ_2/μ_1	600	587	278	324
μ_3/μ_2	900	843	417	425
μ_4/μ_3	1,200	1,062	556	555

*From White and Randolph (1987)
**Theoretical calculations

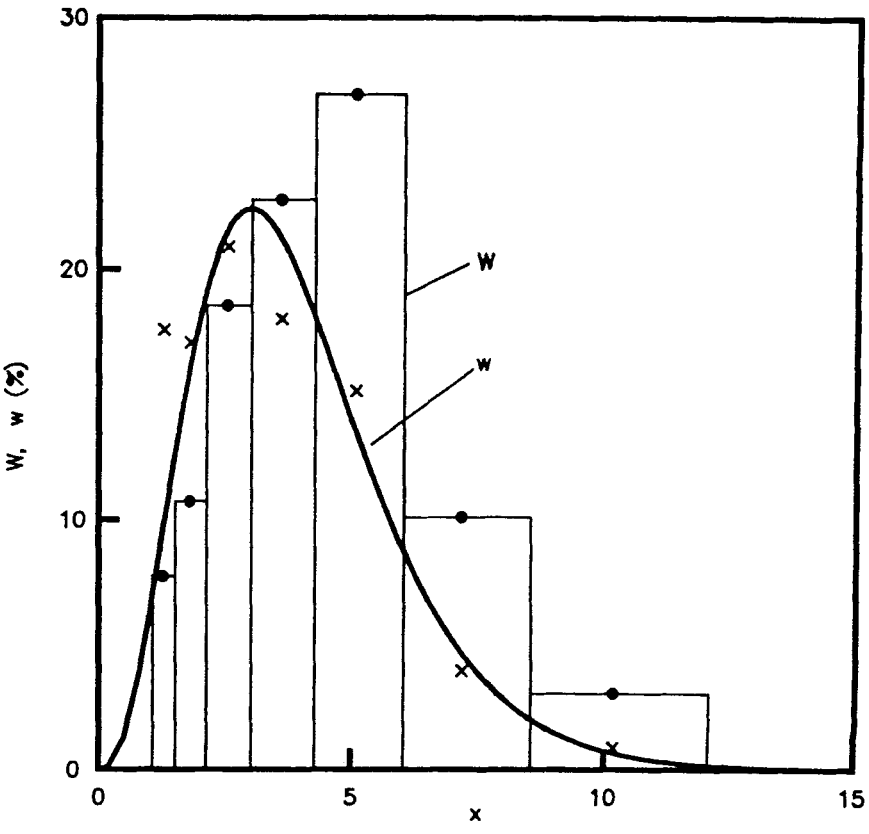

Figure 1. Weight density and differential weight distribution Glauber Salt.
From White and Randolph (1987)

interrelate kinetic information obtained from solution and solid side information in batch crystallization experiments (Tavare, 1987).

Notation

e_p = relative root mean square error based on observed population density, %
e_{pl} = as above, based on observed log population density, %
e_w = as above, based on observed weight density, %
G = growth rate, m/s
k_v = shape factor
L = crystal size, m
$\bar{L}$ = mean size, $= G\tau$, m
$\bar{L}_w$ = weight mean size, m
M_T = magma density, kg/kg
n = population density, n^o/kg · m
n^o = nuclei population density, n^o/kg · m
N = cumulative number oversize, n^o/kg
w = normalized weight density function, %
W = normalized differential weight distr., %
x = size, $L/\bar{L}$
μ_j = jth moment of CSD, n^o · m/kg solvent
ρ_c = crystal density, kg/L
ρ = solution density, kg/L
τ = mean residence time, s

Literature cited

Tavare, N. S., "Batch Crystallizers: a Review," *Chem. Eng. Commun.*, **61**(1–6), 259 (1987).

White, E. T., and A. D. Randolph, "Graphical Solution of the Material Balance Constraint of MSMPR Crystallizers," *AIChE J.*, **33**(4), 686 (Apr., 1987).

N. S. Tavare
Dept. of Chemical Engineering
Univ. of Manchester Inst. of Science and Technology
Manchester M60 1QD, England

Reply:

Tavare has recalculated the Glaubers salt crystallization data of White and Randolph (1987) using the population density plot method and has found similar results (Table 1), thereby further confirming the utility of this widely used method. The calculations were done both with and without the tangency (selfconsistency) constraint, giving similar results. Excellent results were also obtained for a set of simulated data using these methods. The resulting errors for the simulated data (Table 1) are artificial, being only of the order of the computer roundoff error. A more useful test may have been to analyse "noisy" simulated data, with typical experimental error levels added.

However, the alternative attempts to evaluate the parameters by the moments matching method gave poor results for both sets of data, particularly when the lower moments were used. To explain this, it is worthwhile to consider the nature of the size distribution resulting from the usual sizing techniques.

Nature of size distribution

For an ideal MSMPR crystallizer (Randolph and Larson, 1988), the normalized number size distribution in terms of dimensionless size, $x = L/\bar{L}$, is given by

$$f(x) = n/n_o = \exp(-x) \qquad (1)$$

while the normalized mass (volume) distribution is

$$f_m(x) = x^3 \exp(-x) \qquad (2)$$

Most particle sizers use size intervals that increase on a logarithmic (geometric, constant ratio) scale. For example, the fine series of sieves increase in aperture by $\sqrt{2}$ and the coarse series by $\sqrt{2}$, while the electronic sensing zone instruments have sizes arranged in submultiples of doublings. The amount collected in each interval depends upon the size of the interval. To visualise this, the above distributions may be converted to a log size basis, where $y = \ln(x)$, as

$$f(y) = x \exp(-x) \qquad (3)$$

$$f_m(y) = x^4 \exp(-x) \qquad (4)$$

Equations 3 and 4 are plotted in Figure 1. A linear scale is shown for the density function in (a) and a log scale in (b). These plots show the relative amounts (number or mass) that would be collected in the various size fractions, which increase by a constant ratio. Thus Figure 1 shows that the greatest number will be collected in a size interval which includes $x = 1$, ie., $L = \bar{L} = G\tau$. For larger and smaller sizes, lesser numbers will be collected. For mass measurements, the plot shows that the sieve including $x = 4$, ie., $L = 4G\tau$, will contain most mass.

It can be seen that 16 fine series sieves, or eight coarse, covering $x = 0.72$ to 11.6, a 16-fold increase in size, will include 99% of the mass of the distribution. The amount in the end sieves would be less than 5% of that in the greatest. In a practical sieve analysis for an MSMPR crystallizer, it is unlikely that more sieves than this would be used. The Glaubers salt results of White and Randolph used seven coarse series sieves (with x from 1 to 8.5). Tavare used 23 fine series sieves for his simulated results, but this is not a practical case.

With counting sizers, a much wider size range is possible (Figure 1). If the minimum acceptable count per channel is 1% of the largest count, a 2000 fold range of sizes is possible (from $x = 0.004$ to 8). Not all of this range is necessary, nor can the lower end always be measured, as it may be beyond the lower size limit of the sizer. Usually a restricted range is chosen which is most convenient for both the material and the machine operation.

It is also noted that the size range most accurate for mass fraction measurements (roughly $x = 1$ to 10) does not overlap greatly the range most convenient for number counting devices. Often, dif-

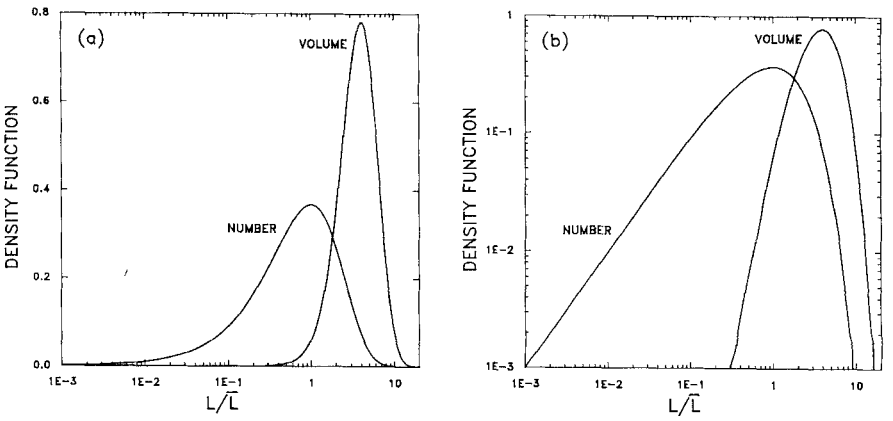

a. Density functions on linear scale *b. Density function on log scale*

Figure 1. Number and volume (mass) density distribution functions for an MSMPR crystallizer on a log size basis.

ferent size ranges will result from sizing done by counting, and that done by sieving.

Moments matching method

The moments matching method is very dependent on the end ("tail") values of the distribution. The population density plot method merely requires enough observations to give an accurate estimate of the slope of the line. The moments matching method, however, requires all observations over the full size range.

For the Glaubers salt results, the smallest sieve used corresponded to approximately $x = 1$. From the Figure it can be seen that half the numbers are below this value. If these are all lumped in the mid-size of the "bottom" sieve, considerable error will result. This explains the poor results for the lower moments calculated for this material. Higher moments are less affected by the lower sizes and better agreement is obtained.

For the simulated data, with x from 0.14 to 6.1, there are tailing problems at both ends. Over 10% of the mass is beyond the larger sieve and if this is "lumped" into the top sieve, serious errors will result with the higher moments. Likewise, as seen from the figure, a considerable fraction (13%) of the numbers will be beyond the finer size and lumping of these will give errors in the lower moments.

Where moments need to be estimated, as in batch crystallizers, we have had some success with a technique where we fit the tails approximately by an exponential distribution and then add mathematical corrections based on these. The method is somewhat tedious as points toward either end of the distribution have to be used to estimate the "time constants" of the approximation. For MSMPR crystallizers there seems little advantage in using moments matching, since the population density plot method is so useful.

We would not recommend the moments matching method for MSMPR crystallizer analysis.

Literature cited

Randolph, A. D., and M. A. Larson, *Theory of Particulate Processes,* 2nd ed., Academic Press, New York (1988).

White, E. T. and A. D. Randolph, "Graphical Solution of the Material Balance Constraint of MSMPR Crystallizers," *AIChE J.*, **33**(4), 686 (Apr., 1987).

E. T. White
Dept. of Chemical Engineering
Univ. of Queensland
Brisbane, Australia 4068

A. D. Randolph
Dept. of Chemical Engineering
Univ. of Arizona
Tucson, AZ 85721